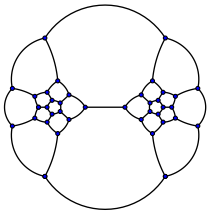

Proceedings of the 4th Croatian Combinatorial Days
CroCoDays 2022
September 22 – 23, 2022

ISBN: 978-953-8168-63-5
DOI: 10.5592/CO/CCD.2022.02

Solving the dimer problem on Apollonian gasket

Tomislav Došlić and Luka Podrug

Abstract

For any three circles in the plane where each circle is tangent to the other two, the Descartes' theorem yields the existence of a fourth circle tangent to the starting three. Continuing this process by adding a new circle between any three tangent circles leads to Apollonian packings. The fractal structures resulting from infinite continuation of such processes are known as Apollonian gaskets. Close-packed dimer configurations on such structures are well modeled by perfect matchings in the corresponding graphs. We consider Apollonian gaskets for several types of initial configurations and present explicit expressions for the number of perfect matchings in such graphs.

1 Introduction

Configurations of close-packed dimers are among the most important objects of study in statistical physics. Also called Kekulé structures in chemical, and perfect matchings in mathematical literature, they serve as useful and (in may cases) tractable models of, among other things, adsorption processes of diatomic molecules on various types of substrates. In that context, the most interesting cases are two-dimensional surfaces with regular structure which are best described by finite portions of two-dimensional infinite lattices. For the simplest case of the square lattice, the exact solution has been known since the early works of Kasteleyn [5] and Temperley and Fisher [4, 12]. (Here by exact solution we mean explicit expressions for all quantities of interest in such problems, such as their growth-rate, entropy, and per-dimer molecular freedom.) For a brief survey of results for some other 2D lattices we refer the reader to [13].

In recent years much attention has been given to another class of lattices or networks, answering thus a need to model processes on fractal-like substrates. The best known example of such lattices is, certainly, the Serpiński gasket. For an accessible

(Tomislav Došlić) University of Zagreb Faculty od Civil Engineering, Croatia, tomislav.doslic@grad.unizg.hr

(Luka Podrug) University of Zagreb Faculty od Civil Engineering, Croatia, luka.podrug@grad.unizg.hr

introduction we refer the reader to [2] and references therein. In this paper we are concerned with related structures which arise from Apollonian packings of circles in the plane and which are known as Apollonian gaskets. Apollonian gaskets are fascinating objects; see, for example, [10] for some beautiful illustrations and for their geometric and number-theoretic properties. They have already attracted significant attention of researchers both in graph theory and in statistical physics. For example, their Tutte polynomials and spanning trees were investigated in [8, 14], while Ising and magnetic models on them were studied in [1, 11] by employing transfer matrices and numerical methods. In this paper we study them from the graph-theoretical point of view and present explicit formulas for the number of close-packed dimer configurations by computing the number of perfect matchings in the corresponding graphs.

In the next section we start from Apollonian packings and introduce the Apollonian gaskets as fractals arising from iterating the packings. Along the way we introduce the necessary graph-theoretic terminology and state some preliminary results. In Section 3 we use those results to present explicit formula for the number of close-packed dimer configurations in a given stage of one particular Apollonian gasket which is, in a sense, canonical. In Section 4 we generalize our findings to some other Apollonian gaskets. The paper is concluded by a short section in which we establish universality of entropy in all Apollonian gaskets and indicate some possible directions for future research.

2 Definitions and preliminary results

Apollonian gasket is a fractal that starts with a number of circles, usually arranged so that each circle is tangent to at least three, but sometimes more, other circles. Construction of the n^{th} level, or the n^{th} iteration, of an Apollonian gasket consists of adding more circles so that every new circle touches exactly three circles in the $(n-1)^{\text{st}}$ level. The number of circles inscribed depends on the number of starting circles and their initial configuration. Radius of each new circle is determined by Descartes' theorem which states that four circles that are tangent to each other at six distinct points with curvatures k_1, k_2, k_3 and k_4 satisfy the following relation:

$$(k_1 + k_2 + k_3 + k_4)^2 = 2(k_1^2 + k_2^2 + k_3^2 + k_4^2). \tag{1}$$

Here the curvature of a circle is the reciprocal value of its radius, i.e., $k = \frac{1}{r}$. Note that equation (1) has two solutions. If one of them is negative, then the corresponding circle touches the other three from inside, otherwise, from outside of a circle. As an example, Figure 1 demonstrates one possible starting configuration of an Apollonian gasket. The curvatures of starting circles uniquely determine curvatures of circles in all subsequent iterations.

Graphs are one of the most fundamental mathematical objects. They naturally appear in many mathematical models, and in this paper we present one such model. More precisely, we consider close-packed dimer configurations on Apollonian gaskets and model them by perfect matching in the corresponding graphs. For the reader's convenience, we state some basic definitions. A *graph* is an ordered pair $G = (V, E)$,

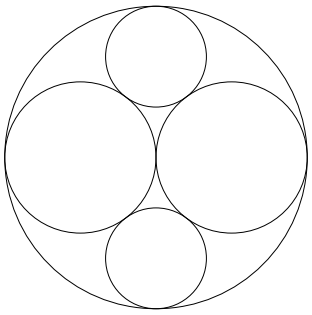

Figure 1: Initial configuration of an Apollonian gasket with circle curvatures -1, 2 and 3.

where $V = V(G)$ stands for a non-empty set of vertices, and $E = E(G)$ is the set of edges. We say that vertices u and v are *adjacent* if there is an edge connecting them, i.e., edge $uv \in E(G)$. For a given vertex v, the number of other vertices adjacent to it is called the *degree* of v. The largest degree in G is denoted by $\Delta(G)$. If all vertices of a graph G have the same degree k, we say that G is *k-regular*. A *perfect matching* in a graph G is a subset $M \subset E(G)$ such that every vertex of G is end-point of exactly one edge in M. The number of perfect matchings of graph G is denoted by $\Phi(G)$. Clearly, a necessary condition for G to have a perfect matching is that the number of vertices must be even. We refer the reader to the classical monograph by Lovász and Plummer [9] for a comprehensive introduction to almost all aspects of matching theory.

Perfect matchings are perfect models for close-packed dimer configurations: The fact that each dimer covers exactly two neighboring sites on the considered substrate is reflected in the fact that each edge of a perfect matching covers two adjacent vertices in the corresponding graph. Further, the non-overlapping requirement for dimers corresponds to the fact that each vertex is incident to exactly one edge of the perfect matching. Finally, the fact that the matching covers every vertex of the graph describes the condition that dimers cover all sites on the substrate, i.e., that they are no empty sites. So the configuration is close-packed.

In order to study dimer configurations on Apollonian gaskets, to each level of an Apollonian gasket we associate a graph obtained in the following manner: each point of tangency is a vertex of the graph and two vertices are adjacent if there is an arc connecting them, provided there are no other tangent points between them. One should note that not every Apollonian gasket produces a graph which has a perfect matching: The graph obtained from Apollonian gasket in Figure 1 has 9 vertices, and thus cannot have a perfect matching. All Apollonian gaskets considered from now on give rise to graphs with perfect matchings. Also, throughout this paper, we will assume that the outside circle in our starting configurations has radius 1.

The *line graph* of a graph G is defined as the graph $L(G)$, where $V(L(G)) = E(G)$, and two edges in $V(L(G))$ are adjacent if they have a common end-vertex in G. The line graph of a cycle is another cycle of the same length, while the line graph of a path is a path with one vertex less. Figures 2 and 3 show two polyhedra, the tetrahedron and the four-sided prism, respectively, and their respective line graphs. Here the edge a in G corresponds to vertex A in $L(G)$, etc.

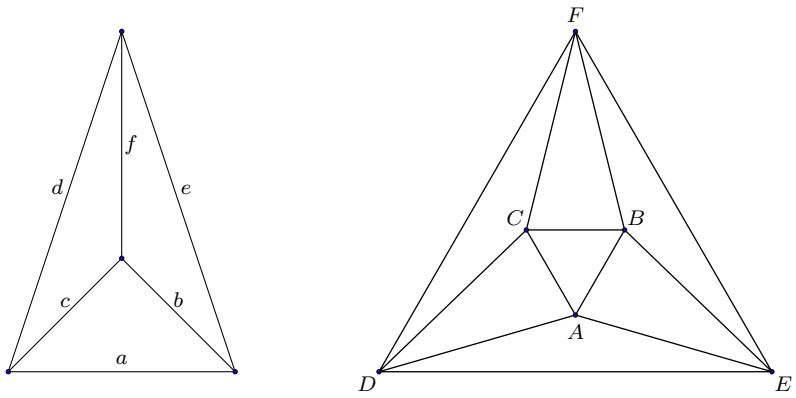

Figure 2: Tetrahedron and its line graph.

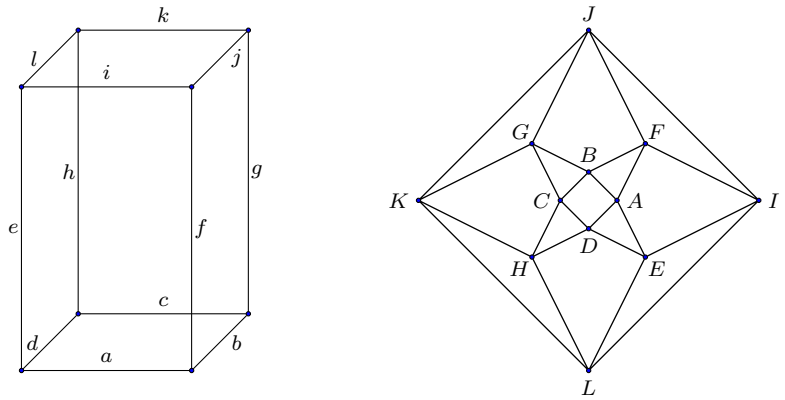

Figure 3: Four-sided prism and its line graph.

To determine a line graph of a given graph is quite straightforward, but the opposite task, to find a graph H such that a given graph G is the line graph of H, can be challenging. It is well-known that not all graphs are line graphs of other graphs. For more details we refer the reader to any textbook on graph theory.
It turns out that in some cases there is a simple relationship between the number of vertices and edges of a given graph G and the number of perfect matchings in its line graph $L(G)$. In particular, Dong, Yan and Zhang [3] proved the following result:

Theorem 1. *Let G be connected graph with n vertices and m edges, where m is even. If $\Delta(G) \leq 3$, then $\Phi(L(G)) = 2^{m-n+1}$.*

We will use this result to obtain the number of perfect matchings of graphs obtained from some configurations of Apollonian gaskets. We start from the case that is, in a way, canonical.

3 Tetrahedron - the canonical case

Let $\mathcal{A}_n$ denote an Apollonian gasket after n iterations and $|\mathcal{A}_n|$ the number of its circles. We denote the initial state of an Apollonian gasket $\mathcal{A}$ by $\mathcal{A}_1$.

Our canonical configuration consists of three starting circles having equal radii $2\sqrt{3}-3$ and one outside circle with radius 1. Figure 4 shows the initial state and the first two iterations of the corresponding Apollonian gasket. They have 4, 8 and 20 circles, respectively. Since the n^{th} iteration adds $4 \cdot 3^{n-2}$ new circles, for $n \geq 2$, the overall number of circles in $\mathcal{A}_n$ is given by

$$|\mathcal{A}_n| = 4 + 4\left(3^0 + \cdots + 3^{n-2}\right) = 2 \cdot \left(3^{n-1} + 1\right).$$

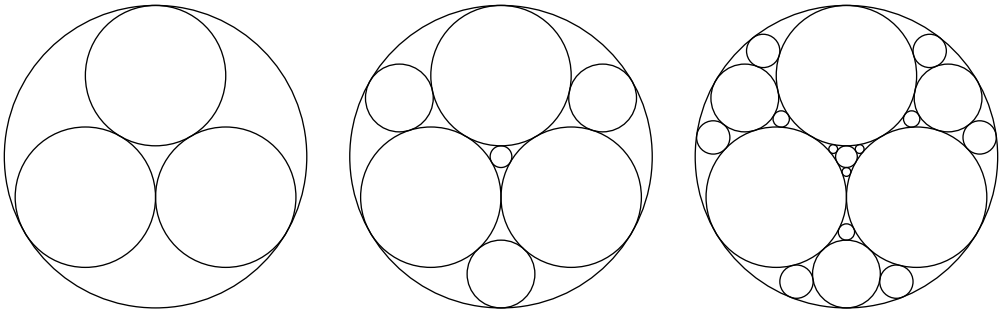

Figure 4: Apollonian gaskets $\mathcal{A}_n$ for $n = 1, 2, 3$.

Now we consider the graphs obtained from this Apollonian gasket. Let A_n denote a graph produced by the n^{th} level of $\mathcal{A}_n$. Then A_1 is a 4-regular graph with 6 vertices and 12 edges. In the second iteration there are 18 vertices, 36 edges, and the graph is again 4-regular. Since the n^{th} iteration adds $4 \cdot 3^{n-2}$ circles and every new circle is tangent to three previously added circles, the n^{th} iteration adds $4 \cdot 3^{n-1}$ new vertices. So,

$$|V(A_n)| = 6 + 4\sum_{i=1}^{n-1} 3^i = 2 \cdot 3^n.$$

Graphs A_n are shown in Figure 5 for $n = 1, 2, 3$. In is not hard to see that A_n is a 4-

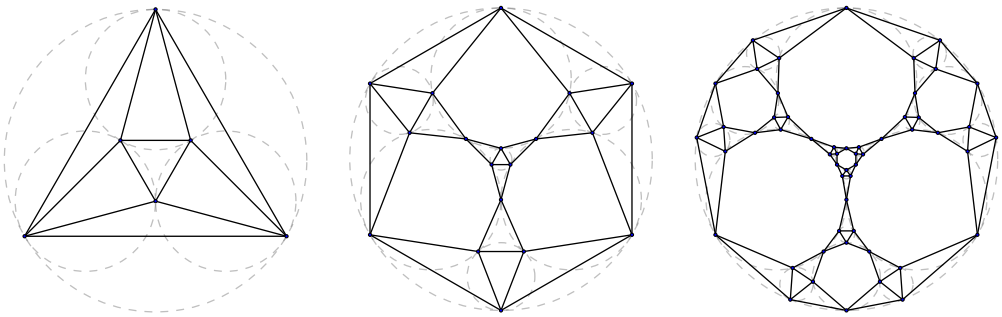

Figure 5: Graphs A_1, A_2 and A_3.

regular graph for every n. Addition of a new circle results in inscribing a new triangle in an already existing one. As shown in Figure 6, after inscribing new triangle shown in red, all new and old vertices have four neighbors. Thus, 4-regularity is preserved. It follows that the number of edges is $|E(A_n)| = 4 \cdot 3^n$.
One can see that A_1 is the octahedron, the line graph of tetrahedron, so we are motivated to ask whether other A_n also appear as line graphs of some related graphs.

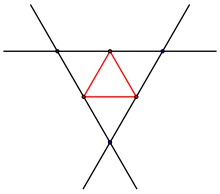

Figure 6: Inscribing a new triangle preserves 4-regularity.

We turn our attention to tetrahedron and start truncating it at its vertices. In every iteration we truncate every vertex of the graph constructed so far (Fig. 7). (Here we do not make distinction between a polyhedron and its graph, but there is no danger of confusion.) Let T_n denotes the graph obtained from the tetrahedron after $n-1$ iterations. Graph T_1 is non-truncated tetrahedron and has 4 vertices. To obtain T_2, we truncate every vertex and every vertex produces 3 vertices. Hence, $|V(T_n)| = 4 \cdot 3^{n-1}$. There are 6 edges in graph T_1 and n^{th} iteration brings $3|V(T_{n-1})|$ new edges. Hence,

$$\begin{aligned} |E(T_n)| =& 6 + 4 \cdot 3^1 + \cdots + 4 \cdot 3^{n-1} \\ =& 2 \cdot 3^n \end{aligned}$$

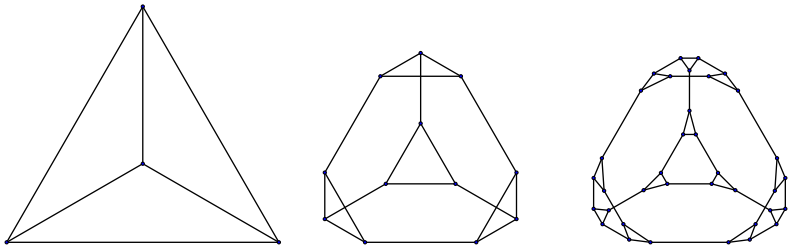

Figure 7: Graphs T_1, T_2 and T_3.

In the next lemma we establish the crucial connection between graphs A_n and T_n.

Lemma 1. $L(T_n) = A_n$.

Proof. The proof is by induction. The base of induction is true, as demonstrated in Figure 2. Graphs isomorphic to A_1, A_2 and A_3 are shown in Figure 8, where their fractal nature is more clear. As we stated, adding new circle results in a subdivision of graph A_n. More precisely, a new triangle is inscribed in an already existing one, thus producing four new triangles. The middle one of those four triangles is not further divided, but the other three are. The triangles that are to be divided are not hard to determine. The leftmost and the rightmost triangle with vertex at the top are divided in every iteration because the middle triangle with top vertex denotes the uppermost of the three original circles, and left and right of that circle is where we add new circles in every iteration. Since some triangles presents circles and other present blank spaces between them, no two divided triangles can share an edge. In that manner, all triangles that will be divided in next iteration are determined. The triangles that will be divided in the next iteration are the colored ones in Figure 8.

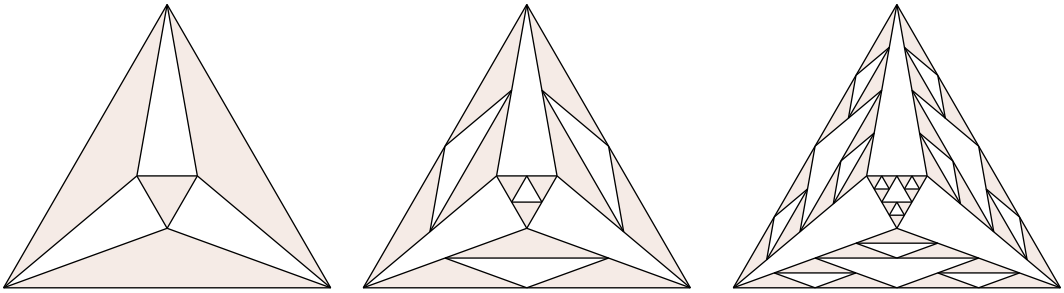

Figure 8: Graphs A_1, A_2 and A_3 with colored triangles that will be divided in the next iteration.

On the other hand, T_n is a 3-regular graph, and every triplet of edges that share a vertex forms a triangle in the corresponding line graph. We say that the vertex is represented by this triangle. Is is not hard to see that graphs shown in Figure 8 are also line graphs of T_1, T_2 and T_3, respectively, as truncating a common vertex inscribes a new triangle in the triangle that represents that vertex. The operation of truncating a vertex and inscribing a triangle in the line graph is shown in Figure 9. The left panel of Figure 9 shows newly-added edges, and the right part shows the corresponding vertices in the line graph, both marked red. We just need to show that triangles which represent vertices of T_n are precisely those colored triangles in Figure 8. First note that two triangles that share an edge in the line graph $L(T_n)$ cannot both represent a vertex. We consider three triangles in line graph that share top vertex. Since $|V(T_n)| = 4 \cdot 3^{n-1}$, there are at least $4 \cdot 3^{n-1}$ triangles in $L(T_n)$. The middle triangle can not represent a vertex, otherwise some vertices would have triangles with shared edge. Thus, alignment of triangles corresponds to Figure 8, and that concludes our proof.

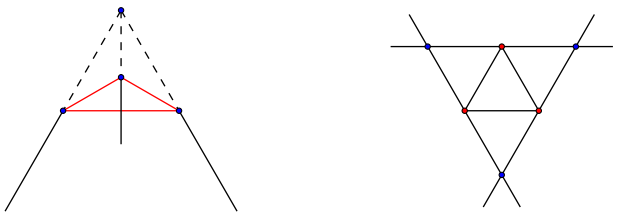

Figure 9: Truncation of a vertex in T_n and its effect in the line graph.

□

Figure 10 demonstrates the connection between graphs T_2 and A_2, more precisely, the fact that $L(T_2) = A_2$.
Now, by Lemma 1 we have $L(T_n) = A_n$ and $\Delta(T_n) = 3$, thus Theorem 1 is applicable to our graphs. Hence we can state the main result of this section.

Theorem 2.

$$\Phi(A_n) = 2 \cdot 4 \cdot 3^{n-1}.$$

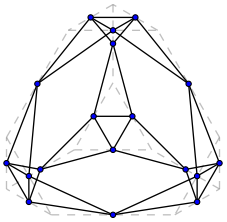

Figure 10: $L(T_2) = A_2$.

4 Other Apollonian gaskets

As we stated above, the initial number and the alignment of circles can vary. There are many different Apollonian packings yielding graphs with perfect matchings, and we here consider some possible simple alignments. Our first example starts with five circles, four with radius $\sqrt{2}-1$ and central one with radius $3-2\sqrt{2}$. As before, in each iteration we add circles in blank spaces between them. First three iterations of this gasket are shown in Figure 11. Similar as before, by B_n we denote a graph

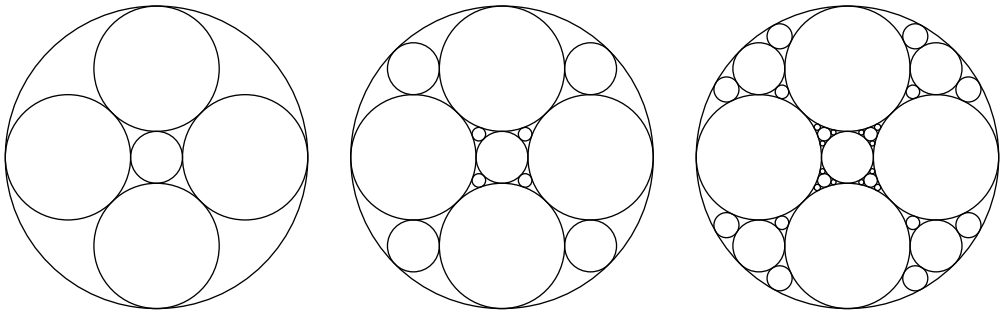

Figure 11: An Apollonian gasket starting with 5 circles.

obtained after $(n-1)^{\text{st}}$ iteration. Graph B_1 is 4-regular, it has 12 vertices and hence, 24 edges. There are $8 \cdot 3^{n-2}$ new circles in the n^{th} iteration that produce $8 \cdot 3^{n-1}$ new vertices. So graph B_n has

$$|V(B_n)| = 12 + 8 \cdot 3 + \cdots + 6 \cdot 3^{n-1} = 4 \cdot 3^n$$

vertices. Thus, it has $|E(B_n)| = 8 \cdot 3^n$ edges. Graphs isomorphic tor B_1, B_2 and B_3 are shown in Figure 12. Again, their fractal nature is clearly visible, because in each iteration, adding new circles in Apollonian gasket produces inscribed triangles in the corresponding graph. As before, B_n is 4-regular for every n.

As in the previous section, we want to identify a family of graphs P_n whose line graphs are graphs B_n. We start with a four-sided prism P_1, shown in Figure 3. Graph P_1 is 3-regular, it has 8 vertices and 12 edges. Furthermore, let P_n denote the starting prism which is truncated $n-1$ times. Every iteration has $8 \cdot 3^{n-1}$ vertices, and since truncation preserves 3-regularity, we have $|E(G)| = 4 \cdot 3^n$. Figure 3 shows the mapping $E(P_1) \to V(L(P_1))$ where edge a on the left corresponds to vertex A on the right, etc. So, $L(P_1) = B_1$. Since truncating a vertex produces same result as it did with tetrahedron, same arguments can be applied to prove that $L(P_n) = A_n$.

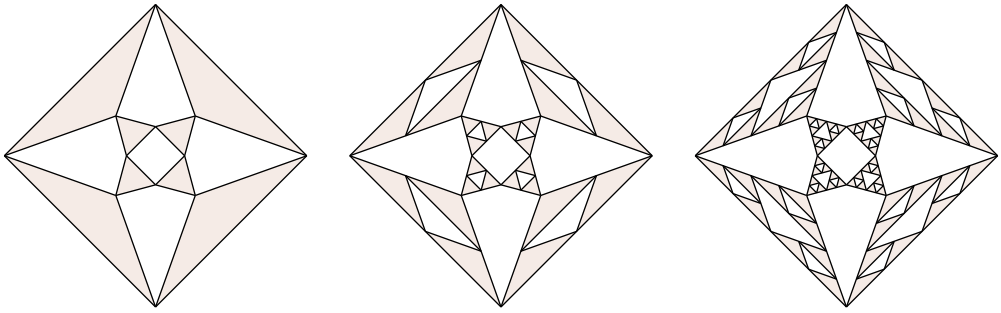

Figure 12: Graphs of initial levels of an Apollonian gasket starting with 5 circles.

Since graphs P_n satisfy assumptions of Theorem 1, we can compute the number of perfect matchings for this class of Apollonian gaskets:

Corollary 1.

$$\Phi(B_n) = 2 \cdot 16^{3^{n-1}}.$$

The Apollonian gasket we have just considered, the one defined by circle curvatures -1 and $1+\sqrt{2}$, can be generalized in a straightforward way. Instead of four circles whose centers are vertices of a square, we can start with m circles whose centers are vertices of regular polygon with m vertices, where $m \geq 4$ is an even integer. As before, let the radius of the outside circle be 1, and let R denote the radius of m circles. The central circle of radius r touches each of those m circles. Since $\sin\left(\frac{\pi}{m}\right) = \frac{R}{R+r}$ and $r + 2R = 1$, we have

$$R = \frac{\sin\left(\frac{\pi}{m}\right)}{1 + \sin\left(\frac{\pi}{m}\right)}.$$

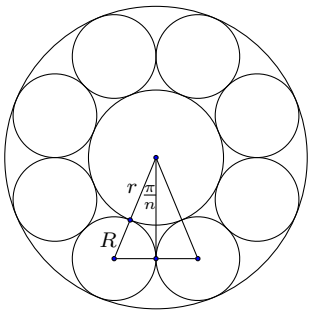

Figure 13: Graph of an Apollonian gasket starting with 9 circles.

We denote the n^{th} iteration of this Apollonian gasket configuration by $\mathcal{A}_n^m$ and the corresponding graph by A_n^m. The graph A_1^m has $3m$ vertices and since it is 4-regular, it has $6m$ edges. With every iteration we add $2m \cdot 3^{n-2}$ circles, hence, $2m \cdot 3^{n-1}$ new vertices. The overall number of vertices is now $V(A_n^m) = m3^n$ and the overall number of edges is $E(A_n^m) = 2m \cdot 3^n$. As we are interested in the number of perfect matchings of graph A_n^m, we only consider cases with m even, otherwise there are no perfect matchings.

By applying the same reasoning as in the previous cases, one can show that A_n^m is the line graph of $n-1$ times truncated m-sided prism, denoted by P_m^n. Again, the graph P_n^m is 3-regular and it has $2m\cdot 3^{n-1}$ vertices and $m\cdot 3^n$ edges. Since $\Delta(P_m^n)=3$ and m is even, by Theorem 1, we have:

Corollary 2.

$$\Phi(A_n^m) = 2\cdot 2^{m\cdot 3^{n-1}}.$$

We notice that our results apply also to $\mathcal{B}=\mathcal{A}^4$.

5 Universality of entropy

We conclude the paper with a few quick glances back to our original problem.
First, we notice that our canonical tetrahedral case could be brought within the framework of the gaskets generated by even-sided prisms by writing its growth rate $4^{3^{n-1}}$ as $2^{2\cdot 3^{n-1}}$ and observing that it fits the pattern $2^{m\cdot 3^{n-1}}$ followed by their growth rates. Hence, the tetrahedron could be considered in this context as an "honorary" even-sided prism.
Our second glance back is toward entropies. The *entropy* of a lattice is defined as the limit of the ratio of the logarithm of the number of perfect matchings and the length of a perfect matching when the number of sites tends to infinity. Hence,

$$\mathcal{E}(\mathcal{G}) = \lim_{n\to\infty} \frac{2\ln \Phi(G_n)}{|V(G_n)|},$$

where by G_n we denote the graph corresponding to the n^{th} level of a gasket $\mathcal{G}$. From our results it immediately follows that the entropy of $\mathcal{A}^m$ does not depend on m.

Corollary 3.

$$\mathcal{E}(\mathcal{A}^m) = \frac{\ln 4}{3}.$$

Hence, while the growth rates depend strongly on m, the corresponding entropy seems to be universal. This fact also implies the universality of the quantity known as per-dimer molecular freedom, defined as

$$W(\mathcal{G}) = e^{\mathcal{E}(\mathcal{G})}.$$

When the considered dimer configurations are not close-packed, i.e., when one deals with monomer-dimer configurations, all quantites of interest become much more difficult to determine; see, for example, a recent paper concerned with generalized Tower of Hanoi graphs [7]. It would be interesting to examine whether some progress could be made by using the approach of the present paper.
Our last remark is concerned with a recent paper by Li *et al.* [6] which extends the line of research of Dong *et al.* by looking at the dimer problem at the vertex-edge graphs of cubic graphs. It would be interesting to find classes of fractal lattices for which the results by Li *et al.* would provide compact explicit solutions of the type presented here.

Acknowledgements

Partial support of Slovenian ARRS (Grant no. J1-3002) is gratefully acknowledged by T. Došlić.

References

[1] R. F. S. Andrade, H. J. Herrmann, Magnetic models on Apollonian networks, *Phys. Rev. E* 71 (2005) 056131.

[2] J. A. Anema, K. Tsougkas, Counting spanning trees on fractal graphs and their asymptotic complexity, *J. Phys. A: Math. Theor.* 49 (2016) 355101.

[3] F. Dong, W. Yan, F. Zhang On the number of perfect matching of line graphs, *Discrete Appl. Math.* **161**, 794–801 (2013).

[4] M. E. Fisher, Statistical mechanics of dimers on a plane lattice, *Phys. Rev.* 124 (1961) 1664–1672.

[5] P. W. Kasteleyn, The statistics of dimers on a lattice, *Physica* 27 (1961) 1209–1225.

[6] S. Li, D. Li, W. Yan, On the dimer problem of the vertex-edge graph of a cubic graph, *Discrete Math.* 346 (2023) 113427.

[7] W.-B. Li, S.-C. Chang, Study of dimer–monomer on the generalized Hanoi graph, *Comput. Appl. Math.* 39 (2020) 77.

[8] Y. Liao, Y. Hou, X. Shen, Tutte polynomials of the Apollonian networks, *J. Stat. Mech.* (2014) P10043.

[9] L. Lovász, M. D. Plummer, *Matching Theory*, in: Ann. Discrete Math. vol. 29, North-Holland, New York, 1986.

[10] D. Mackenzie, A tisket, a tasket, an Apollonian gasket, *Amer. Sci.* 98 (2010) 10–14.

[11] M. Serva, U. L. Fulco, E. L. Albuquerque, Ising models on regularized Apollonian networks, *Phys. Rev. E* 88 (2013) 042823.

[12] H. N. V. Temperley, M. E. Fisher, Dimer problem in statistical mechanics – An exact result, *Phil. Mag.* 6 (1961) 1061–1063.

[13] F. Y. Wu, Dimers on two-dimensional lattices, *Int. J. Mod. Phys. B* 20 (2006) 5357–5371.

[14] Z. Zhang, B. Wu, F. Comellas, The number of spanning trees in Apollonian networks, *Discrete Appl. Math.* 169 (2014) 206–213.